Rapid generation of human B-cell lymphomas via combined expression of Myc and Bcl2 and their use as a preclinical model for biological therapies

Ilya Leskov PhD[1,5], Christian P. Pallasch MD[1,2,3,5], Adam Drake PhD[1], Bettina P. Iliopoulou PhD [1], Amanda Souza B.S.[1], Ching-Hung Shen PhD[1], Carmen D. Schweighofer MD[2,4], Lynne Abruzzo MD[3], Lukas P. Frenzel MD[2,3], Clemens M. Wendtner MD[2,3], Michael T. Hemann PhD[1] and Jianzhu Chen PhD[1]

Running Title: Humanized Mouse Model of “Double-hit” Lymphoma

[1] Koch Institute for Integrative Cancer Research and Department of Biology, Massachusetts Institute of Technology, Cambridge, MA 02139, USA

[2] Department I of Internal Medicine, Center of Integrated Oncology, University of Cologne, Cologne, Germany

[3] Cluster of Excellence for Cellular Stress Response in Aging-Associated Diseases (CECAD), University of Cologne, Cologne, Germany.

[4] Department of Hematopathology, UT M.D. Anderson Cancer Center Houston, TX 77030, USA

[5] These authors contributed equally to this work

Correspondence should be addressed to MTH (hemann@mit.edu) or JC (jchen@mit.edu)

The authors declare no competing financial interest.

Abstract

While numerous mouse models of B cell malignancy have been developed via the enforced expression of defined oncogenic lesions, the feasibility of generating lineage-defined human B cell malignancies using mice reconstituted with modified human hematopoietic stem cells remains unclear. In fact, whether human cells can be transformed as readily as murine cells by simple oncogene combinations is a subject of considerable debate. Here, we describe the development of humanized mouse model of MYC/BCL2-driven “double-hit” lymphoma. By engrafting human hematopoietic stem cells transduced with the oncogene combination into immunodeficient mice, we generate a fatal B malignancy with complete penetrance. This humanized-MYC/BCL2-model (hMB) accurately recapitulates the histopathological and clinical aspects of steroid-, chemotherapy- and rituximab-resistant human “double-hit” lymphomas that involve the MYC and BCL2 loci. Notably, this model can serve as a platform for the evaluation of antibody-based therapeutics. As a proof of principle, we used this model to show that the anti-CD52 antibody alemtuzumab effectively eliminates lymphoma cells from the spleen, liver, and peripheral blood, but not from the brain. The hMB humanized mouse model underscores the synergy of MYC and BCL2 in “double-hit” lymphomas in human patients. Additionally, our findings highlight the utility of humanized mouse models in interrogating therapeutic approaches, particularly human-specific monoclonal antibodies.

Introduction

The accumulation of sequential or simultaneous genetic alterations is a key feature of the development of human malignancies. Deregulated c-MYC and BCL2 together have recently been found to promote the development of so-called “double-hit” high-grade human B-cell lymphomas/leukemias (1-4). Other genes involved in translocations, like BCL6 and CCND1, have also been described, however c-MYC and BCL2 represent the most frequent combination. These “double-hit” lymphomas include patients with various histomorphological classifications such as follicular lymphoma, mantle cell lymphoma, diffuse Large B-cell lymphoma, mature B-cell neoplasia not otherwise specified, Burkitt’s Lymphoma and acute lymphoblastic lymphoma/leukemia (1). “Double-hit” lymphomas represent an estimated 2% of all B-cell malignancies, but they are also the most refractory to therapy (with an average survival of 18.6 months) and represent a major clinical challenge (5-7). Notably, the combination of deregulated c-MYC and BCL2 have been shown by numerous groups to promote a rapid and aggressive pro-B cell malignancy in mice (8-10). These tumors have been used as an effective pre-clinical model, but are not amenable to the analysis of human-specific therapies.

Antibody-based therapies targeting CD20 using rituximab have significantly improved the general patient outcome in B-cell lymphoma patients, however “double-hit” lymphomas do not express or express much reduced levels of CD20 (11, 12). The development of more personalized and effective therapies including antibody based approaches for treating patients harboring “double-hit” lymphomas has been hampered by the lack of diagnostic awareness, therapeutic options and suitable pre-clinical models for therapeutic development.

While conventional transgenic models can be quite effective at assessing the response of tumors to general cytotoxic agents, they cannot be used to evaluate the efficacy of human-specific therapeutic antibodies. This includes murine models in which the human antigen has been introduced (13). A more recent approach to modeling hematologic malignancies is to engraft immunodeficient mice with genetically modified human hematopoietic stem cells (HSCs) (14). Here, we used this approach to determine whether we could generate a B cell malignancy that phenocopies human "double-hit" lymphomas. We then used this humanized mouse model as a preclinical platform for examining the efficacy of cytotoxic and human-specific antibody based therapies.

Results and Discussion

To model "double-hit" lymphoma in humanized mice, we engineered c-MYC^{T58A} and BCL2 overexpression in human B-lineage cells. Here, c-MYC^{T58A} is an oncogenic allele of Myc found in transforming avian alleles of Myc, as well as many cases of human Burkitt's lymphoma (15-17). Following *in vitro* expansion, human cord-blood derived CD133^{+} HSCs were transduced with lentiviruses expressing GFP alone, GFP-BCL2, GFP-MYC^{T58A} or GFP-c-MYC ^{T58A}-BCL2 under the control of a B-cell specific Eμ-enhancer/CD19-promoter (18-21). Transduced HSCs were then engrafted into sub-lethally irradiated NOD-scid Il2Rg$^{-/-}$ (NSG) mice (10^6 per recipient) (Figure 1A) (22). Four weeks after reconstitution, human CD45^{+} leukocytes were readily detected in the peripheral blood of reconstituted mice, suggesting humanization of the hematopoietic system.

Nine weeks after reconstitution, 10.8% of human $CD45^+$ cells in the peripheral blood were GFP^+ in mice that received the GFP virus-transduced HSCs (referred to as GFP mice, 2A). No GFP^+ cells were observed in GFP-MYC^{T58A} mice, while 33.2% of human $CD45^+$ cells were GFP^+ in GFP-BCL2 mice – with comparable cell stage distribution throughout B-cell developmental (Figure 1B; Supplemental Tables 1 and 2). Additionally, no tumor or clinical sign of malignant transformation was ever detected in GFP, GFP-MYC^{T58A} or GFP-BCL2 mice during the same observation period. Compared to GFP-only mice GFP-BCL2 developed a mild hyperplasia of human B-cells over the course of several months (Figure 1C), however no clinical symptoms arose from the increased number of B-cells in these mice. Furthermore, transfer of GFP-sorted cells from GFP-BCL2 mice failed to induce tumors in secondary recipient mice.

In contrast, nearly all human $CD45^+$ cells were GFP^+ in in mice that received the GFP-c-MYC^{T58A}-BCL2 virus-transduced HSCs (referred to as hMB mice)(Figure 1B). With time, hMB mice gradually lost weight, developed massive splenomegaly and occasionally ataxia and died on average 12 weeks post-HSC transfer (Figure 2A,B). Histological examination revealed the presence of uniform blast-like cells with multiple prominent nucleoli and mitotic figures in the peripheral blood, bone marrow, and spleen of the hMB mice; tumor cells were also present in the liver, kidneys, muscles, mediastinum, retroperitoneum and, notably, the leptomeningeal spaces in the brain (Figure 2C-F, Supplemental Figure 1). Flow cytometry analysis showed that the majority of splenocytes (11) from symptomatic hMB mice were positive for GFP as well as human CD45, CD10, CD19, IL-7Rα, CD22, cytoplasmic CD79a, cytoplasmic IgM, and TdT, but low for CD20 and negative for surface IgM (Figure 3A) - an immunophenotype most

characteristic of a pre-B cell lymphoma/leukemia and consistent with previous immunophenotyping of patient "double-hit" lymphoma cells. Additionally, expression of the introduced transgenes MYC and BCL2 could be observed in all lymphoma cells derived from hMB mice (Supplemental Figure S2). Southern blot hybridization of tumor DNA with a GFP-specific probe revealed either monoclonal or oligoclonal lymphomas (Supplementary Figure 3), suggesting a potential requirement for one or more additional alterations during tumor development.

In order to identify secondary genetic lesions involved in the pathogenesis of the leukemia model we performed karyotyping of primary cells derived from three hMB mice after disease onset. In one mouse, we failed to detect a second cytogenetic alteration. A trisomy 7 bearing subclone (formal karyotype: 47, XX, +7 [8] / 46, XX [14]) was detected in a second hMB mouse (Figure 3B). In the third mouse, we could identify an elongation of chromosome 17p and a subclone bearing an elongation of chromosome 12p (formal karyotype 46, XX, add(17)(q25.3)[13] / 46, XX, idem, add(12)(p13.3)[8] / 46, XX[4]) (Figure 3C). However, the elongation at chromosome 12p did not involve the ETV locus, as characterized by FISH probing. Thus, the formation of leukemic clones does not require an obligate defined secondary major chromosomal loss or translocation. However, we identified trisomy chromosome 7 in 1 out of 3 karyotyped lymphomas. This alteration is commonly found in patient-derived "double-hit" lymphomas/leukemias (2).

To verify that the disease arising in hMB mice indeed represented a *bona fide* malignancy, we transplanted 10^6 hMB lymphoma cells purified from primary hMB mice into unirradiated

secondary NSG recipients. GFP^+ lymphoma cells were detectable in the peripheral blood of the secondary recipients after 14 days, and onset of disease symptoms was evident after 21-28 days. Onset of disease in transplanted mice is dependent on total numbers of injected cells, as transplantation of $2x10^5$ cells gave rise to disease in recipient after 4-6 weeks. However, in all cases, the resulting disease was clinically and histologically identical to that in primary donor hMB mice. Thus, the coordinated expression of MYC and BCL2 are capable of producing a completely penetrant early B cell malignancy.

The generation of large cohorts of secondary mice bearing synchronously appearing hMB lymphomas allowed us to examine the effects of a diverse set of therapeutics on a genetically defined lymphoma. Treatment was initialized upon the presentation of leukemic outgrowth or development of the above-mentioned clinical symptoms. When used individually, dexamethasone showed no effect (Figure 4A). Doxorubicin had a statistically significant, but minimal, effect on reducing tumor burden, while cytarabine and total body irradiation only had a modest effect (Figure 4A). A partial response could be observed with cyclophosphamide, including some reduction in brain infiltrating malignant cells (Figure 4B). However, survival of mice was not significantly improved after cyclophosphamide chemotherapy (Figure 4C). Thus, these lymphomas were both steroid and chemotherapy resistant. Surprisingly an anti-BCL2 targeted approach towards hMB lymphoma cells, using the BCL2 inhibitor ABT-737, also failed to promote lymphoma cell apoptosis (Supplemental Figure S4). Importantly, this humanized mouse model of “double-hit” lymphoma allowed us to assess the efficacy of human-specific antibody-based therapeutics. We took advantage of the hMB lymphoma cells’ expression of CD52 (Figure 3E) and tested the human CD52-specific therapeutic antibody

alemtuzumab (Campath-1H, Genzyme). Alemtuzumab treatment significantly prolonged overall survival of lymphoma mice (Figure 4C, $p<0.01$ in all experiments). In contrast, an anti-CD20 treatment approach using rituximab (MabThera, Roche) failed to induce treatment response (Supplemental Figure 5). Rituximab failure in this context is consistent with low CD20 expression by these tumors, an immunophenotype consistent with that of patient-derived “double-hit” lymphomas (11).

Notably, seven days after the start of alemtuzumab treatment, tumor cell burden was reduced approximately 100-fold in the peripheral blood, the spleen, and the liver (Figure 4D). However, tumor cell burden was not reduced in the brain. Using fluorescently labeled alemtuzumab *in vivo*, we observed antibody bound to GFP^+ lymphoma cells in the spleen, while no specific staining could be detected in the brain (Figure 4E-G) Thus, alemtuzumab cannot efficiently target lymphoma cells in the central nervous system, probably because the antibody molecules do not cross the blood-brain barrier, and all alemtuzumab-treated mice eventually succumbed to a relapse of the malignant disease.

Here, we have developed a humanized mouse model of “double-hit” lymphoma by directing coordinated overexpression of c-MYC and BCL2 in human HSC-derived B lineage cells. Notably, development of these lymphomas was dependent upon a combination of both the MYC and BCL2 oncogenes, as neither individual oncogene could readily promote malignant growth. In mice, introduction of Eμ-myc and Eμ-bcl2 alteration leads to the very rapid formation of polyclonal lymphomas (10). However, lymphoma formation is not strictly dependent on Bcl2 co-expression (23), as both Eμ-myc and c-Myc^{T58A} mice can eventually

acquire secondary alterations and develop monoclonal or oligoclonal disease. In a human hematopoetic stem cell based system, we show that a single alteration with B-cell overexpression of c-MYC^{T58A} is not sufficient for lymphoma formation within the 6-month period of the experiment. In particular, no GFP-MYC B cells were detected in the humanized mouse, suggesting that the residual pro-apoptotic features of MYC^{T58A} (24) result in the ablation of these cells prior to the occurrence of pro-survival mutations. It remains unclear whether the MYC^{T58A} allele makes any significant contribution to tumor development in this context, but the uniformly high levels of BCL2 seen by western blot in tumor samples suggests the presence of a high apoptotic threshold limiting tumor lymphoma development. It also remains to be determined how frequently c-MYC is mutated in “double-hit” lymphomas, however the common presence of these mutations on translocated Myc alleles suggests that “double-hit” lymphomas that are initiated by MYC translocations will show similar MYC alterations.

The GFP-BCL2 construct induced an increased persistence of non-transformed B-cells, but no B-cell malignancies – a phenotype that mirrors murine phenotypes of Bcl-2-immunoglobulin transgenic mice (25). While methodological differences exist between these “humanized” experiments and similar murine efforts, including both viral and promotor choice, these data suggest that perhaps an additional “hit” beyond MYC and BCL2 expression is necessary to induce a malignant transformation or clinical phenotype in human cells. Further work, including retroviral insertion site analysis will be required to identify cooperating alterations in this context.

Human cells are thought to show greater resistance towards malignant transformation than murine cells. For example, in mouse cells, perturbation of only two pathways has been shown to be sufficient to induce malignant transformation, while up to six pathways need to be altered in corresponding human cells (26). Thus, it was unexpected to see a robust malignant phenotype with 100% penetrance in the hMB model. This stands in contrast to other recent studies involving the introduction of defined oncogenic perturbations into human hematopoietic stem cells, where engraftment of these cells into immunodeficient recipient mice has resulted in variable disease penetrance or non-malignant phenotypes (27-31). For example, leukemic transformation was reported following introduction of the MLL-fusion proteins MLL-AF9 and MML-ENL (14) into HSCs, whereas MLL-AF4 and AML-ETO failed to induce malignant transformation (32, 33). Thus, the oncogenic synergy of MYC^{T58A} and BCL2 shown in the hMB model underlines their central role as “driving” events in tumor pathogenesis.

The use of a humanized model of lymphoma in preclinical modeling of therapeutic regimens provides several advantages relative to conventional transgenic or murine transgenic models. First, we can generate a *de novo* arising human malignancy not harboring artifacts from extensive tissue culture of cell line-based xenograft approaches. Additionally, these tumors can be modified rapidly *ex vivo* and, unlike many xenograft tumors, are highly amenable to transplantation into recipient mice. As a proof of principle we show that antibody-mediated targeting of CD52 can produce potent anti-tumor effects in this model. This monoclonal anti-CD52 antibody has been in clinical use for relapsed CLL and is currently under investigation in several clinical trials for other malignancies (34). Treatment outcome in this humanized

model may better predict the effects of antibody-based therapy in patients. Thus far alemtuzumab-containing protocols have not been specifically addressed to “double-hit” lymphomas, however analogous to recent trials in T-NHL, a CHOP-alemtuzumab approach specifically addressed to “double-hit” lymphomas might represent a promising strategy despite the severe toxicity profile of the antibody (35).

Currently, a multitude of novel compounds are in preclinical development for treatment refractory leukemias/lymphomas. However, given the low frequency of diagnosed “double-hit” lymphomas, clinical trials for this malignancy are necessarily limited in size and number. Consequently, initial pre-clinical testing involving an accurate humanized mouse model may offer the opportunity to evaluate human-specific antibody and chemo-immunotherapeutic regimens prior to human clinical trials.

Acknowledgements

We thank P. Bak and Herman Eisen for helpful discussions and the Swanson Biotechnology Center for excellent technical support. This work was partly supported by grants from the Marble Family Foundation (to J.C. and M.T.H.), Singapore-MIT Alliance for Research and Technology (to J.C.) and the NIH (R01-CA128803 to M.T.H.). C.P.P. is supported by a research fellowship of the German Research foundation. I.L. was supported in part by the MIT School of Science Cancer Research Fellowship, the Ludwig Academic Graduate Fellowship, and the Medical Scientist Training Program (Grant Number T32GM007753 from the National Institute Of General Medical Sciences). The content is solely the responsibility of the authors

and does not necessarily represent the official views of the National Institute Of General Medical Sciences or the National Institutes of Health.

Conflict of Interest Disclosures

The authors declare no conflicts of interest.

References

1. Aukema SM, Siebert R, Schuuring E, van Imhoff GW, Kluin-Nelemans HC, Boerma EJ*, et al.* Double-hit B-cell lymphomas. *Blood* 2011 Feb 24; **117**(8)**:** 2319-2331.

2. Snuderl M, Kolman OK, Chen YB, Hsu JJ, Ackerman AM, Dal Cin P*, et al.* B-cell lymphomas with concurrent IGH-BCL2 and MYC rearrangements are aggressive neoplasms with clinical and pathologic features distinct from Burkitt lymphoma and diffuse large B-cell lymphoma. *The American journal of surgical pathology* 2010 Mar; **34**(3)**:** 327-340.

3. Hasserjian RP, Ott G, Elenitoba-Johnson KS, Balague-Ponz O, de Jong D, de Leval L. Commentary on the WHO classification of tumors of lymphoid tissues (2008): "Gray zone" lymphomas overlapping with Burkitt lymphoma or classical Hodgkin lymphoma. *Journal of hematopathology* 2009 Jun 27.

4. Bacher U, Haferlach T, Alpermann T, Kern W, Schnittger S, Haferlach C. Several lymphoma-specific genetic events in parallel can be found in mature B-cell neoplasms. *Genes, chromosomes & cancer* 2011 Jan; **50**(1)**:** 43-50.

5. Tomita N. BCL2 and MYC dual-hit lymphoma/leukemia. *Journal of clinical and experimental hematopathology : JCEH* 2011; **51**(1)**:** 7-12.

6. Li S, Lin P, Fayad LE, Lennon PA, Miranda RN, Yin CC*, et al.* B-cell lymphomas with MYC/8q24 rearrangements and IGH@BCL2/t(14;18)(q32;q21): an aggressive disease with heterogeneous histology, germinal center B-cell immunophenotype and poor outcome. *Modern pathology : an official journal of the United States and Canadian Academy of Pathology, Inc* 2011 Oct 14.

7. Johnson NA, Savage KJ, Ludkovski O, Ben-Neriah S, Woods R, Steidl C*, et al.* Lymphomas with concurrent BCL2 and MYC translocations: the critical factors associated with survival. *Blood* 2009 Sep 10; **114**(11)**:** 2273-2279.

8. Schmitt CA, Lowe SW. Bcl-2 mediates chemoresistance in matched pairs of primary E(mu)-myc lymphomas in vivo. *Blood cells, molecules & diseases* 2001 Jan-Feb; **27**(1)**:** 206-216.

9. Vaux DL, Cory S, Adams JM. Bcl-2 gene promotes haemopoietic cell survival and cooperates with c-myc to immortalize pre-B cells. *Nature* 1988 Sep 29; **335**(6189)**:** 440-442.

10. Strasser A, Harris AW, Bath ML, Cory S. Novel primitive lymphoid tumours induced in transgenic mice by cooperation between myc and bcl-2. *Nature* 1990 Nov 22; **348**(6299)**:** 331-333.

11. Wu D, Wood BL, Dorer R, Fromm JR. "Double-Hit" mature B-cell lymphomas show a common immunophenotype by flow cytometry that includes decreased CD20 expression. *American journal of clinical pathology* 2010 Aug; **134**(2)**:** 258-265.

12. Harrington AM, Olteanu H, Kroft SH, Eshoa C. The unique immunophenotype of double-hit lymphomas. *Am J Clin Pathol* 2011 Apr; **135**(4)**:** 649-650.

13. Hu Y, Turner MJ, Shields J, Gale MS, Hutto E, Roberts BL*, et al.* Investigation of the mechanism of action of alemtuzumab in a human CD52 transgenic mouse model. *Immunology* 2009 Oct; **128**(2)**:** 260-270.

14. Barabe F, Kennedy JA, Hope KJ, Dick JE. Modeling the initiation and progression of human acute leukemia in mice. *Science* 2007 Apr 27; **316**(5824)**:** 600-604.

15. Bhatia K, Huppi K, Spangler G, Siwarski D, Iyer R, Magrath I. Point mutations in the c-Myc transactivation domain are common in Burkitt's lymphoma and mouse plasmacytomas. *Nature genetics* 1993 Sep; **5**(1)**:** 56-61.

16. Smith-Sorensen B, Hijmans EM, Beijersbergen RL, Bernards R. Functional analysis of Burkitt's lymphoma mutant c-Myc proteins. *The Journal of biological chemistry* 1996 Mar 8; **271**(10)**:** 5513-5518.

17. Gu W, Bhatia K, Magrath IT, Dang CV, Dalla-Favera R. Binding and suppression of the Myc transcriptional activation domain by p107. *Science* 1994 Apr 8; **264**(5156)**:** 251-254.

18. Moreau T, Bardin F, Imbert J, Chabannon C, Tonnelle C. Restriction of transgene expression to the B-lymphoid progeny of human lentivirally transduced CD34+ cells. *Molecular therapy : the journal of the American Society of Gene Therapy* 2004 Jul; **10**(1)**:** 45-56.

19. Stern P, Astrof S, Erkeland SJ, Schustak J, Sharp PA, Hynes RO. A system for Cre-regulated RNA interference in vivo. *Proc Natl Acad Sci U S A* 2008 Sep 16; **105**(37)**:** 13895-13900.

20. Zhang CC, Kaba M, Iizuka S, Huynh H, Lodish HF. Angiopoietin-like 5 and IGFBP2 stimulate ex vivo expansion of human cord blood hematopoietic stem cells as assayed by NOD/SCID transplantation. *Blood* 2008 Apr 1; **111**(7)**:** 3415-3423.

21. Giassi LJ, Pearson T, Shultz LD, Laning J, Biber K, Kraus M*, et al.* Expanded CD34+ human umbilical cord blood cells generate multiple lymphohematopoietic lineages in NOD-scid IL2rgamma(null) mice. *Exp Biol Med (Maywood)* 2008 Aug; **233**(8)**:** 997-1012.

22. Shultz LD, Lyons BL, Burzenski LM, Gott B, Chen X, Chaleff S*, et al.* Human lymphoid and myeloid cell development in NOD/LtSz-scid IL2R gamma null mice engrafted with

mobilized human hemopoietic stem cells. *J Immunol* 2005 May 15; **174**(10)**:** 6477-6489.

23. Kelly PN, Puthalakath H, Adams JM, Strasser A. Endogenous bcl-2 is not required for the development of Emu-myc-induced B-cell lymphoma. *Blood* 2007 Jun 1; **109**(11)**:** 4907-4913.

24. Prendergast GC. Mechanisms of apoptosis by c-Myc. *Oncogene* 1999 May 13; **18**(19)**:** 2967-2987.

25. McDonnell TJ, Deane N, Platt FM, Nunez G, Jaeger U, McKearn JP*, et al.* bcl-2-immunoglobulin transgenic mice demonstrate extended B cell survival and follicular lymphoproliferation. *Cell* 1989 Apr 7; **57**(1)**:** 79-88.

26. Rangarajan A, Hong SJ, Gifford A, Weinberg RA. Species- and cell type-specific requirements for cellular transformation. *Cancer cell* 2004 Aug; **6**(2)**:** 171-183.

27. Chung KY, Morrone G, Schuringa JJ, Plasilova M, Shieh JH, Zhang Y*, et al.* Enforced expression of NUP98-HOXA9 in human CD34(+) cells enhances stem cell proliferation. *Cancer Res* 2006 Dec 15; **66**(24)**:** 11781-11791.

28. Wunderlich M, Krejci O, Wei J, Mulloy JC. Human CD34+ cells expressing the inv(16) fusion protein exhibit a myelomonocytic phenotype with greatly enhanced proliferative ability. *Blood* 2006 Sep 1; **108**(5)**:** 1690-1697.

29. Buske C, Feuring-Buske M, Antonchuk J, Rosten P, Hogge DE, Eaves CJ*, et al.* Overexpression of HOXA10 perturbs human lymphomyelopoiesis in vitro and in vivo. *Blood* 2001 Apr 15; **97**(8)**:** 2286-2292.

30. Chung KY, Morrone G, Schuringa JJ, Wong B, Dorn DC, Moore MA. Enforced expression of an Flt3 internal tandem duplication in human CD34+ cells confers properties of self-renewal and enhanced erythropoiesis. *Blood* 2005 Jan 1; **105**(1)**:** 77-84.

31. Schuringa JJ, Chung KY, Morrone G, Moore MA. Constitutive activation of STAT5A promotes human hematopoietic stem cell self-renewal and erythroid differentiation. *J Exp Med* 2004 Sep 6; **200**(5)**:** 623-635.

32. Montes R, Ayllon V, Gutierrez-Aranda I, Prat I, Hernandez-Lamas MC, Ponce L*, et al.* Enforced expression of MLL-AF4 fusion in cord blood CD34+ cells enhances the hematopoietic repopulating cell function and clonogenic potential but is not sufficient to initiate leukemia. *Blood* 2011 Mar 9.

33. Basecke J, Schwieger M, Griesinger F, Schiedlmeier B, Wulf G, Trumper L*, et al.* AML1/ETO promotes the maintenance of early hematopoietic progenitors in

NOD/SCID mice but does not abrogate their lineage specific differentiation. *Leuk Lymphoma* 2005 Feb; **46**(2)**:** 265-272.

34. Wendtner CM, Ritgen M, Schweighofer CD, Fingerle-Rowson G, Campe H, Jager G*, et al.* Consolidation with alemtuzumab in patients with chronic lymphocytic leukemia (CLL) in first remission--experience on safety and efficacy within a randomized multicenter phase III trial of the German CLL Study Group (GCLLSG). *Leukemia* 2004 Jun; **18**(6)**:** 1093-1101.

35. Gallamini A, Zaja F, Patti C, Billio A, Specchia MR, Tucci A*, et al.* Alemtuzumab (Campath-1H) and CHOP chemotherapy as first-line treatment of peripheral T-cell lymphoma: results of a GITIL (Gruppo Italiano Terapie Innovative nei Linfomi) prospective multicenter trial. *Blood* 2007 Oct 1; **110**(7)**:** 2316-2323.

Figure Legends

Figure 1. A humanized mouse model of "double-hit" lymphoma. (**A**) A schematic diagram showing the lentiviral vector in which the human B cell-specific enhancer-promotor controls the expression of GFP, c-MYC, and BCL2, transduction of human hematopoietic stem cells (HSC), and generatioin of humanized mice. The dot-plot shows human CD45 (hCD45) versus murine CD45 (mCD45) staining of peripheral blood mononuclear cells of a representative humanized mouse 9 weeks after reconstitution. **(B)** Peripheral blood mononuclear cells (PBMCs) from NSG mice injected with lentivirally-transduced human HSCs. Peripheral blood was analyzed for hCD45, mCD45 and GFP 9 weeks after engraftment in GFP, GFP-MYC, GFP-BCL2 and GFP-MYC-BCL2 mice (n=5). Histograms show GFP expression gating on human $CD45^+$ cells indicated in Figure 1A. Murine cells are GFP-negative. Percentages of GFP^+ cells are indicated. **(C)** Time dependent development of B-cell hyperplasia in GFP-BCL2 mice. Sublethally irradiated adult NSG mice were engrafted with human $CD133^+$ cells that had been spin-infected with lentivirus expressing either GFP alone or GFP plus BCL2. At the indicated times following engraftment, PBMCs from these mice were analyzed for GFP expression. All cells were gated on human $CD45^+$ cells. Numbers indicate percent cells in the indicated region. Representative data from at least 5 mice are shown

Figure 2: Clinical presentation of the hMB model. (**A**) Kaplan-Meier survival analysis of GFP-control (G; n=9), GFP-BCL2 (GB; n=5), GFP-MYC (GM; n=5) and GFP-MYC-BCL2 (hMB; n=9). (**B**) Representative image of a control (GFP) and a leukemic hMB spleen at week 12 post injection and corresponding representative low-magnification cross-section of a control

(GFP) and a leukemic hMB spleen. (**C-F**) Histomorphological analysis of leukemic mice. (**C**) Bone marrow smear (Giemsa-Wright staining). (**D**) Bone marrow section (H&E staining) with (**E**) Spleen high magnification showing lymphoma blast cells. **(F)** Brain section (H&E staining) showing leptomeningeal infiltration by leukemic blasts.

Figure 3. Flow cytometry analysis of reconstituted mice. **(A)** Flow cytometry analysis of lymphoma cells from spleens of diseased hMB mice. Splenocytes were stained for hCD45 as well as human CD19, CD10, surface IgM (sIgM), CD20, CD52, surface CD22 (sCD22), IL-7Rα, TdT, cytoplasmic IgM (cyIgM), or cytoplasmic CD79a (cyCD79a). Dot plots show GFP versus the indicated surface staining of $hCD45^+$ cells. Histograms show TdT, IL-7Rα, cyIgM and cyCD79a staining of $hCD45^+$ cells (dark line) versus isotype controls (faint lines). Karyotyping of tumors showing (**B**) trisomy 7 and (**C**) an elongation at chromosome 12p. Representative metaphases from a minimum of 22 metaphases per sample are displayed.

Figure 4. Therapeutic modeling in the hMB "double-hit" lymphoma model. (**A**) Secondary transplant mice were treated upon presence of leukemic cells in the peripheral blood at day 21 post transplant (corresponding to day 1 of treatment) with dexamethasone (DEX; 10 mg/kg), doxorubicin (DOX;5 mg/kg), cytarabine (ARA-C;50 mg/kg), total body irradiation (RAD; 5 Gy), cyclophosphamide (CYP; 300 mg/kg) or alemtuzumab (ALEM; 5 mg/kg). Treatment response was assessed at day 7 post treatment by measuring total number of GFP^+ lymphoma cells in the spleen. (**B**) Comparison of tumor burden in peripheral blood, spleen and brain 8 days after initiating cyclophosphamide treatment. GFP^+ lymphoma cells

were counted using the C6 flow cytometer (Accuri Cytometers). Each symbol represents one mouse; average and standard error are shown for each group. P values of indicated comparisons are shown (n.s.=non-significant). (**C**) Kaplan-Meier survival analysis of secondary hMB recipient mice that received intravenous injections of alemtuzumab (Alem., 5 mg/kg) or of vehicle control; 3 injections over 7 days, delivered on days 1, 4, and 7). (**D**) Comparison of tumor burden in different organs 8 days after initiating alemtuzumab treatment. GFP^+ lymphoma cells were counted using the C6 flow cytometer (Accuri Cytometers). Each symbol represents one mouse; average and standard error are shown for each group. P values of indicated comparisons are shown (n.s.=non-significant). (**E**) Visualization of the *in vivo* distribution of alemtuzumab 24 hours following injection into either non-reconstituted NSG mice or NSG mice transferred with hMB lymphoma cells. Mice were injected with 5 mg/kg AlexaFluor750-labeled alemtuzumab and distribution of fluorescence assessed after 6h. Representative scans of healthy control vs. lymphoma hMB mice showing enriched signal from spleen and long bones. **(F)** Alemtuzumab binding to target organs comparing non-transplanted healthy NSG mice to hMB-mice. Brains were dissected from the skull and assessed separately for quantification. Spleens were examined *in situ*. Photon emission from defined region of interest was quantified for spleen and brain (n=6 each). (**G**) Flow cytometry analysis of AlexaFLuor750-alemtuzumab binding to GFP^+ lymphoma cells in the spleen but not in brain parenchyma and submeningeal space. Cells were directly subjected to flow cytometry after organ dissociation

Figure 1

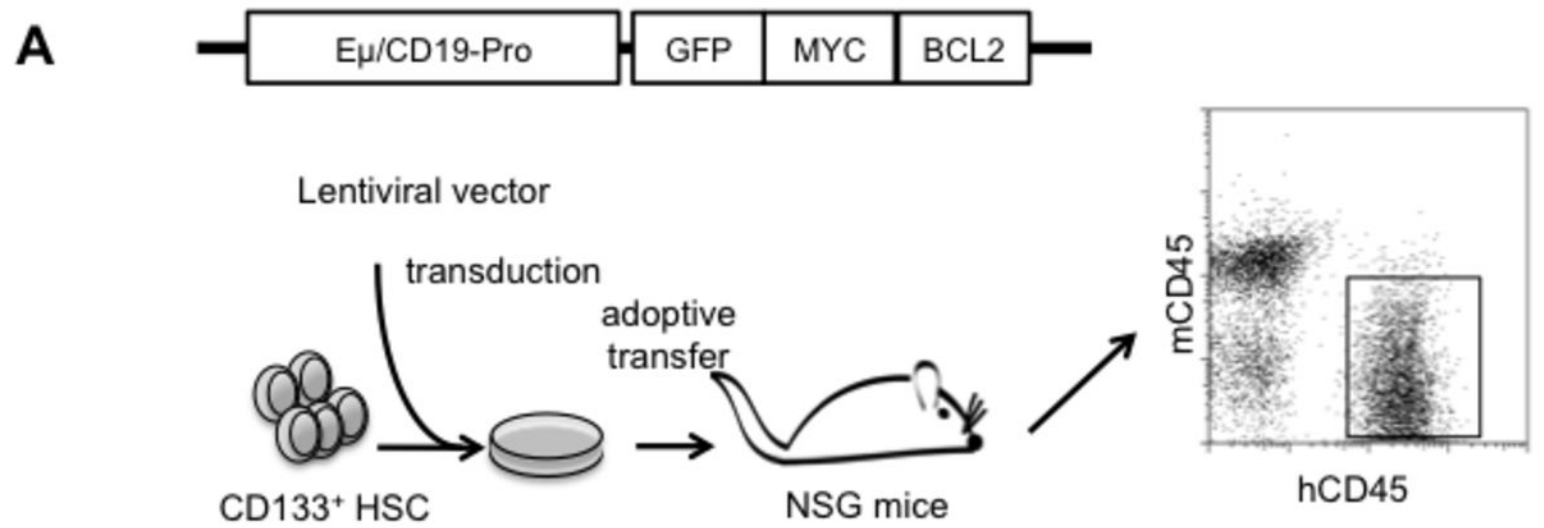
A
Eμ/CD19-Pro
GFP
MYC
BCL2
Lentiviral vector
transduction
adoptive
transfer
CD133+ HSC
NSG mice
mCD45
hCD45

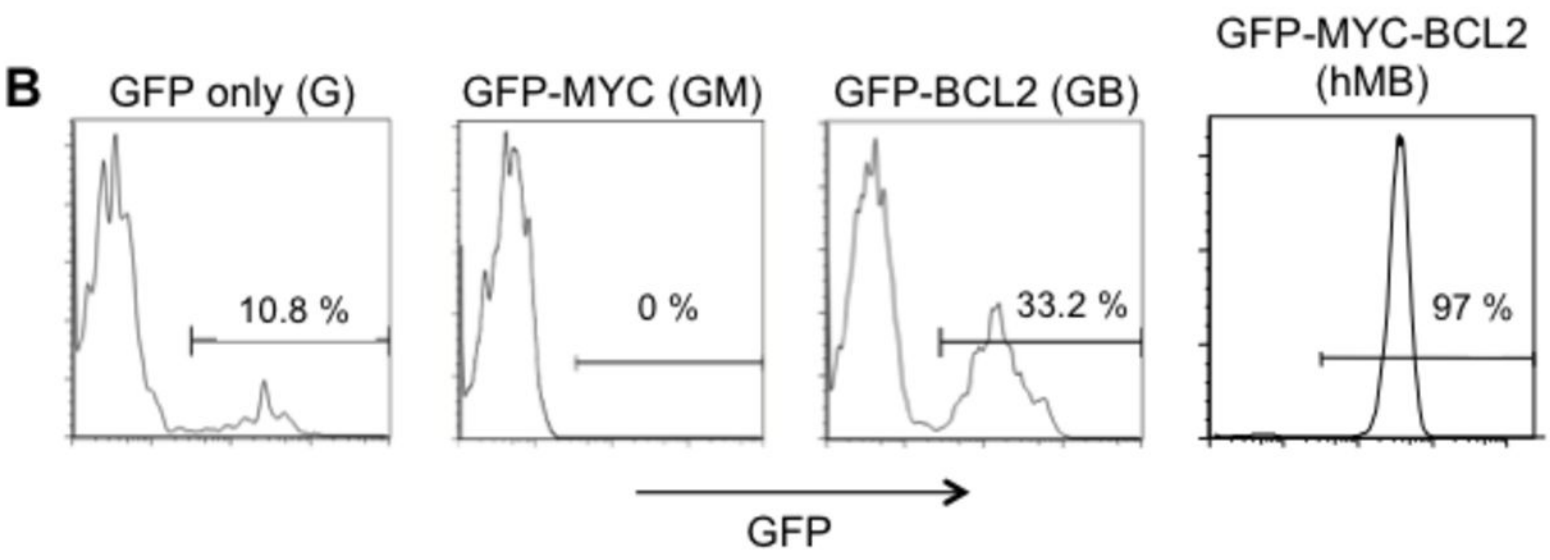
B
GFP only (G)
GFP-MYC (GM)
GFP-BCL2 (GB)
GFP-MYC-BCL2
(hMB)
10.8 %
0 %
33.2 %
97 %
GFP

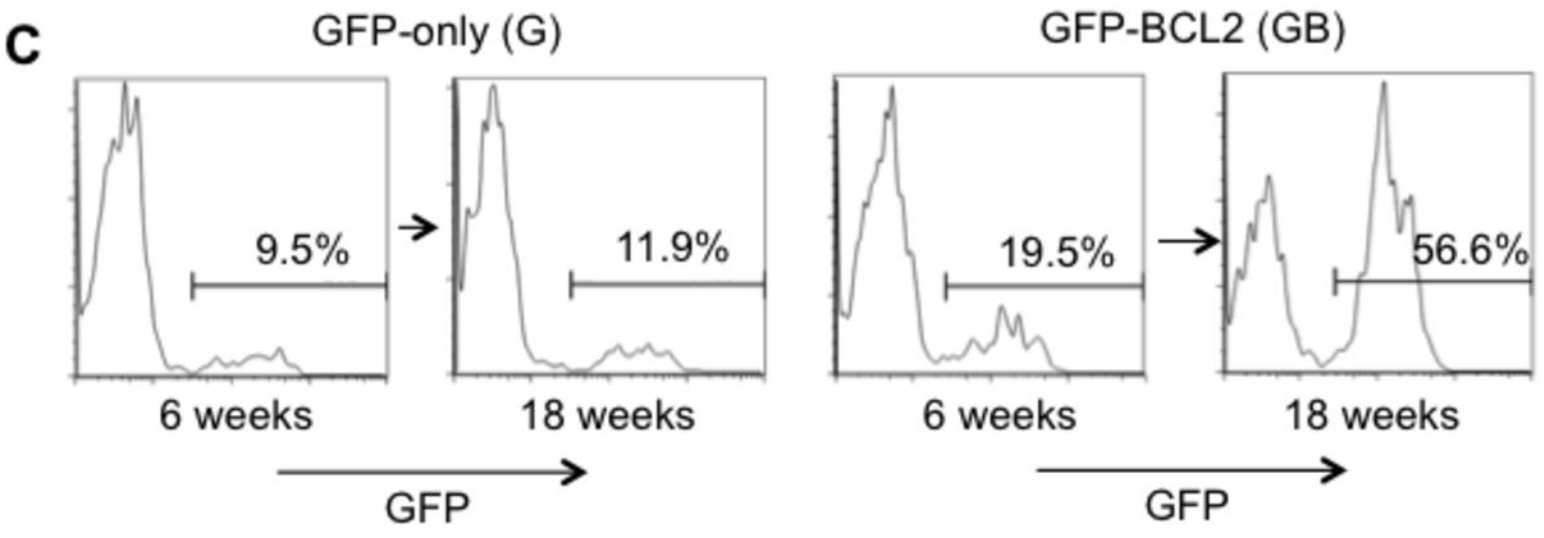
C
GFP-only (G)
GFP-BCL2 (GB)
9.5%
11.9%
19.5%
56.6%
6 weeks
18 weeks
6 weeks
18 weeks
GFP
GFP

Figure 2

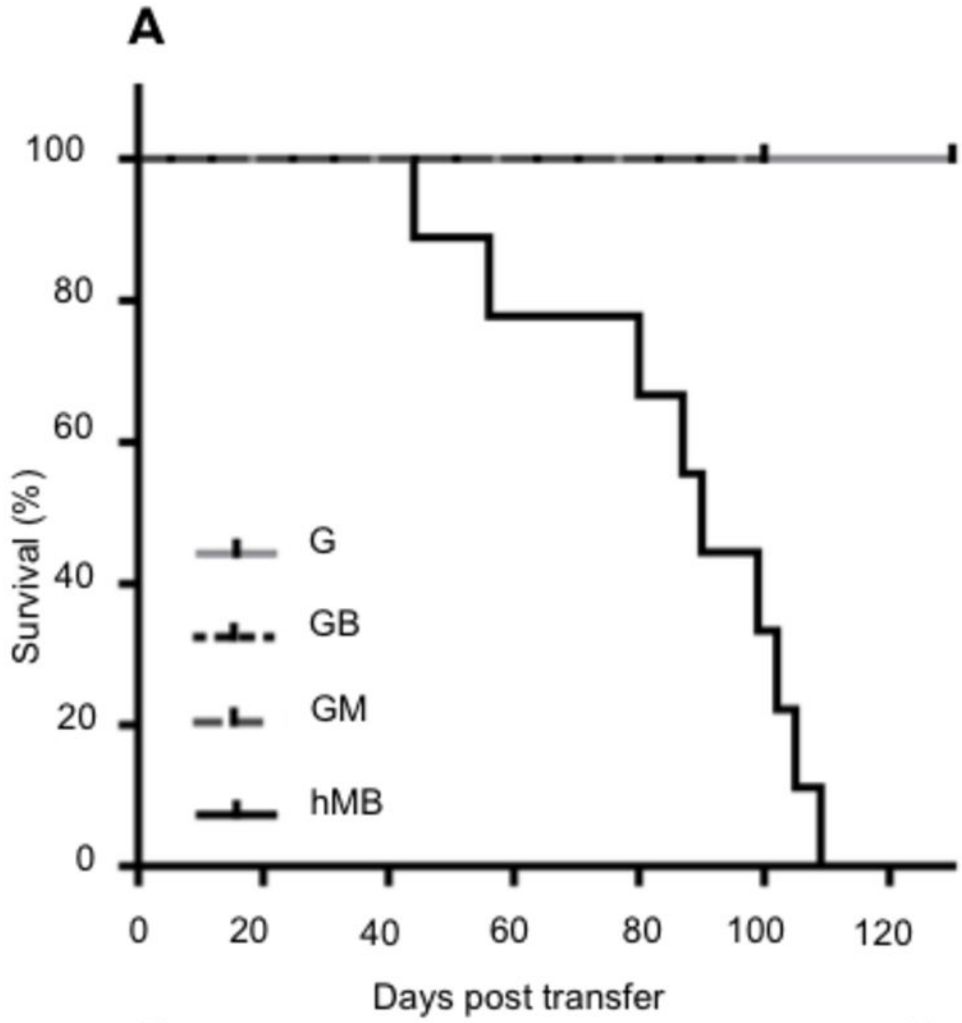
A
100
80
60
40
20
0
Survival (%)
G
GB
GM
hMB
0
20
40
60
80
100
120
Days post transfer

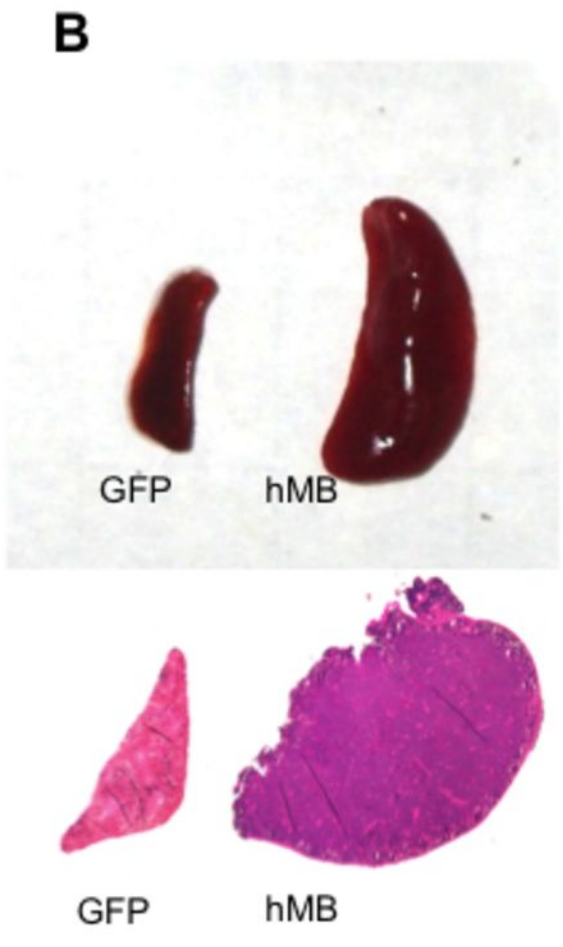
B
GFP
hMB
GFP
hMB

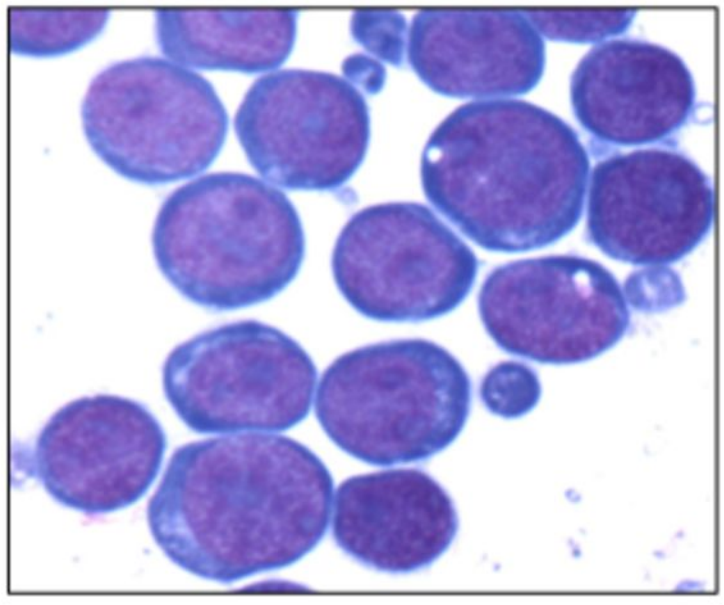
C

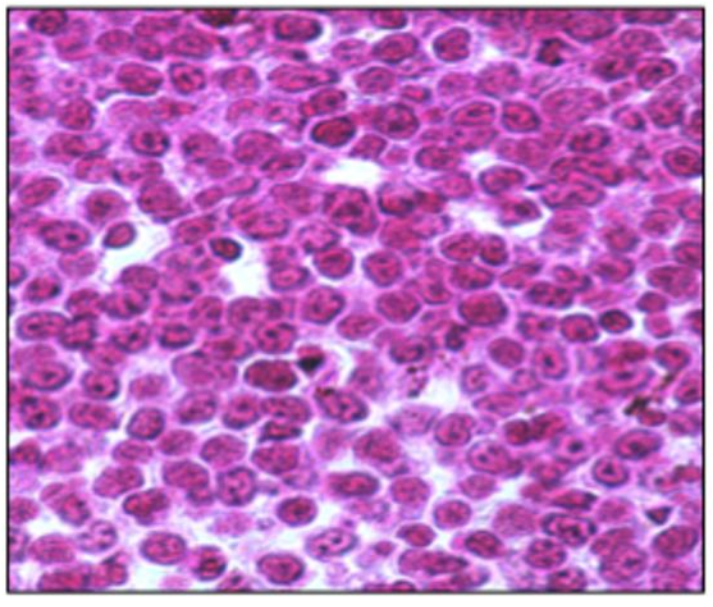
D

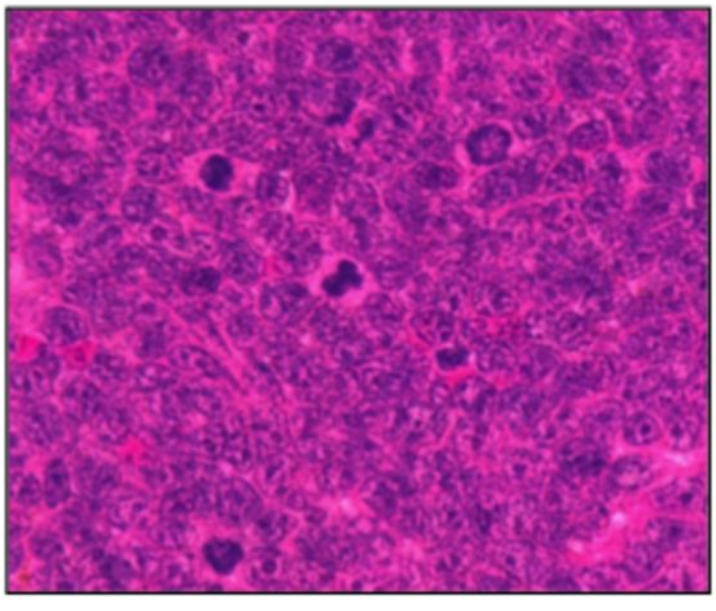
E

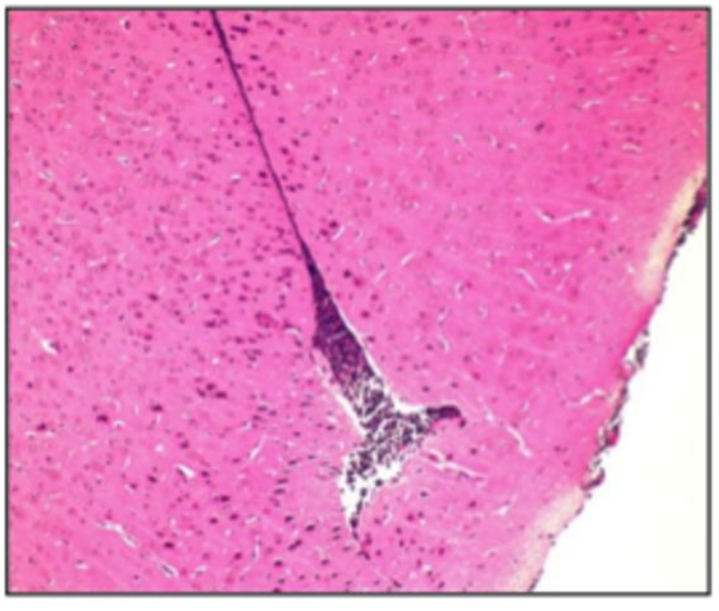
F

Figure 3

A

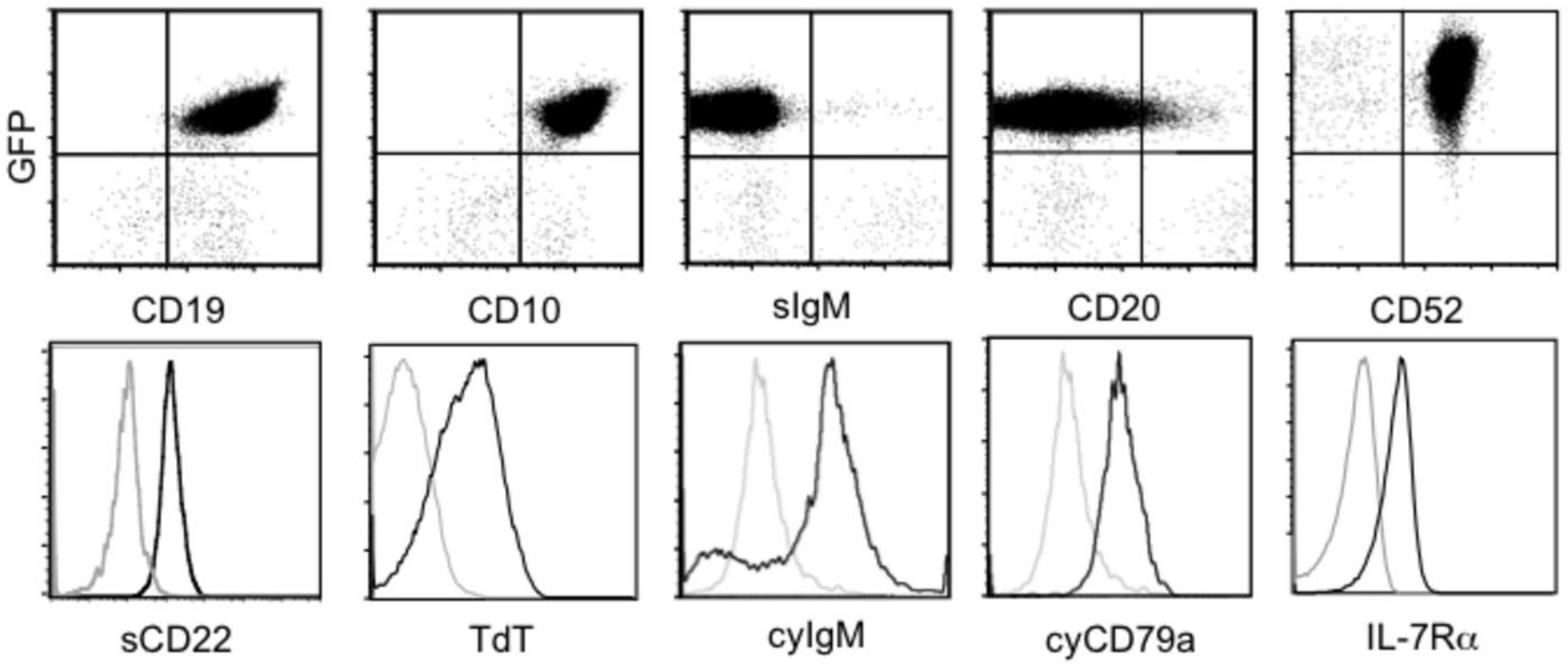
GFP
CD19
CD10
sIgM
CD20
CD52
sCD22
TdT
cyIgM
cyCD79a
IL-7Rα

B

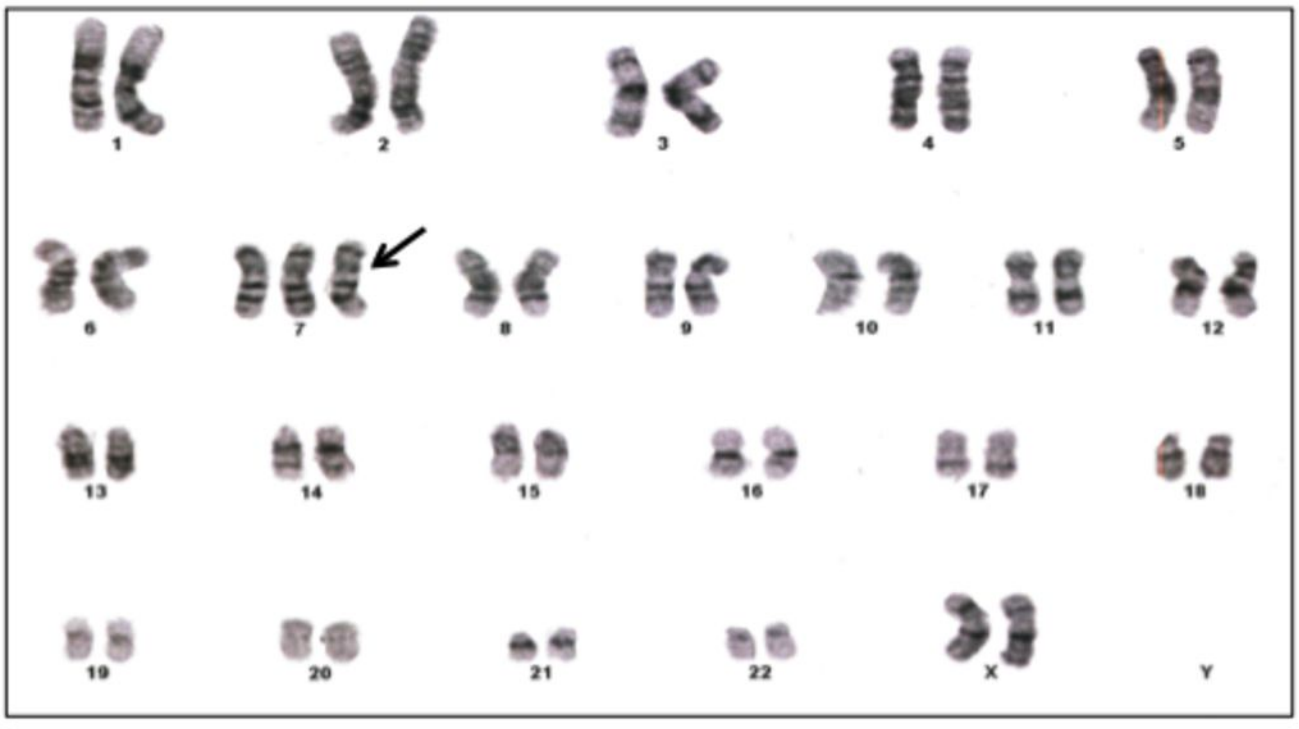
1
2
3
4
5
6
7
8
9
10
11
12
13
14
15
16
17
18
19
20
21
22
X
Y

C

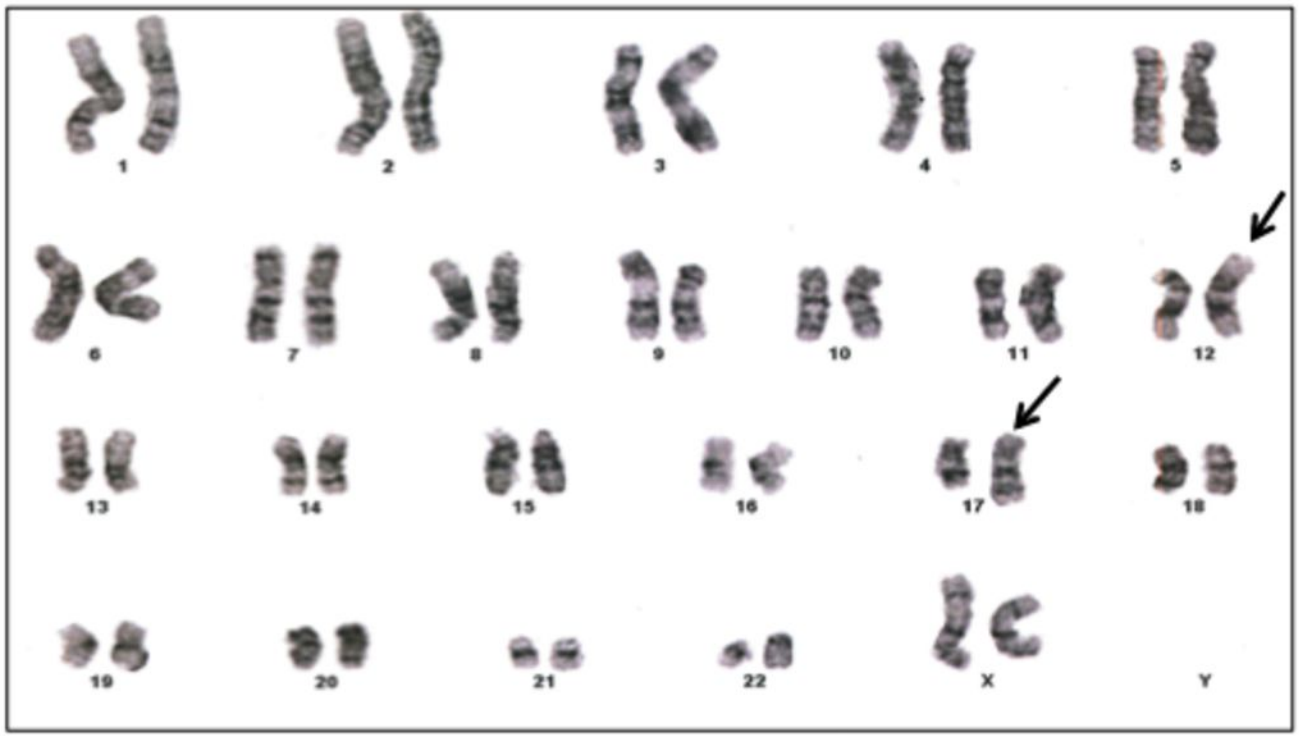
1
2
3
4
5
6
7
8
9
10
11
12
13
14
15
16
17
18
19
20
21
22
X
Y

Figure 4

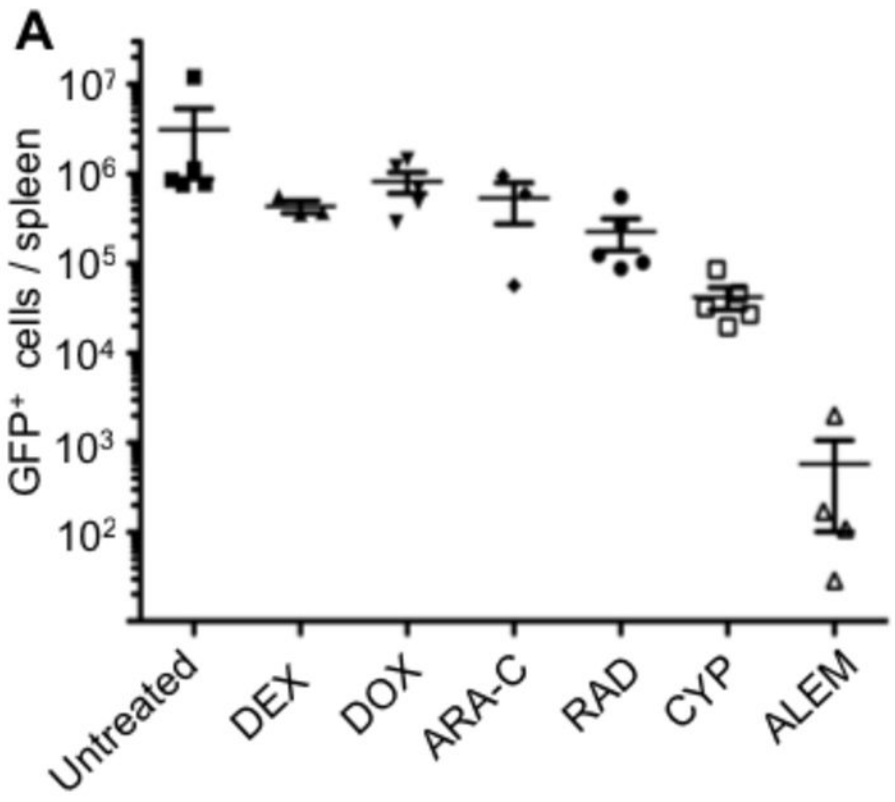
A
GFP+ cells / spleen
10^7
10^6
10^5
10^4
10^3
10^2
Untreated
DEX
DOX
ARA-C
RAD
CYP
ALEM

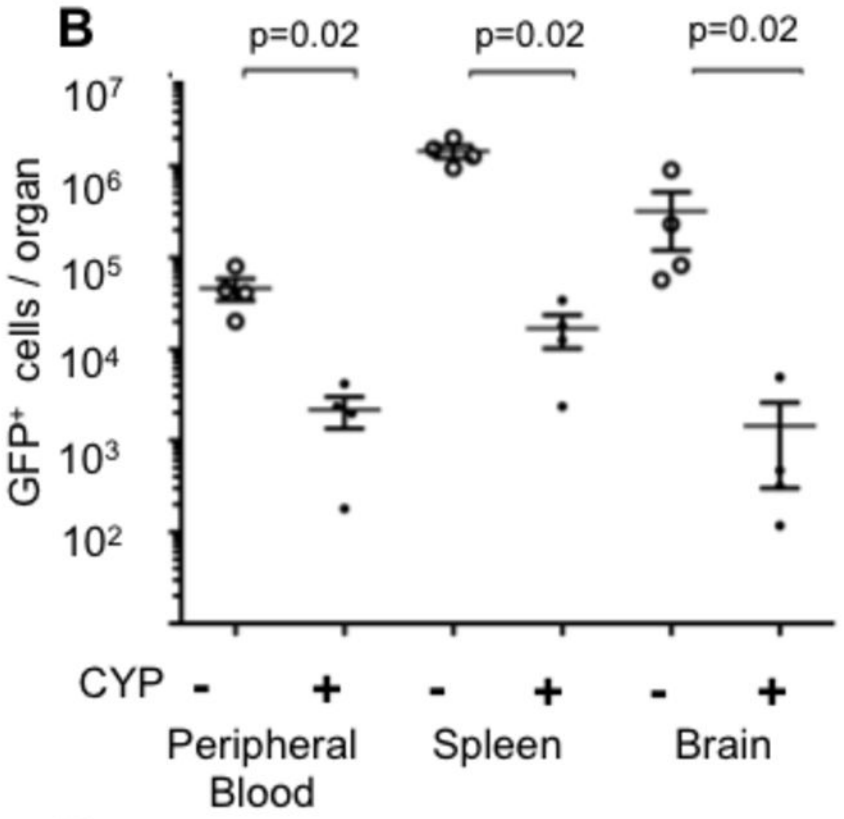
B
p=0.02
p=0.02
p=0.02
GFP+ cells / organ
10^7
10^6
10^5
10^4
10^3
10^2
CYP - + - + - +
Peripheral Blood
Spleen
Brain

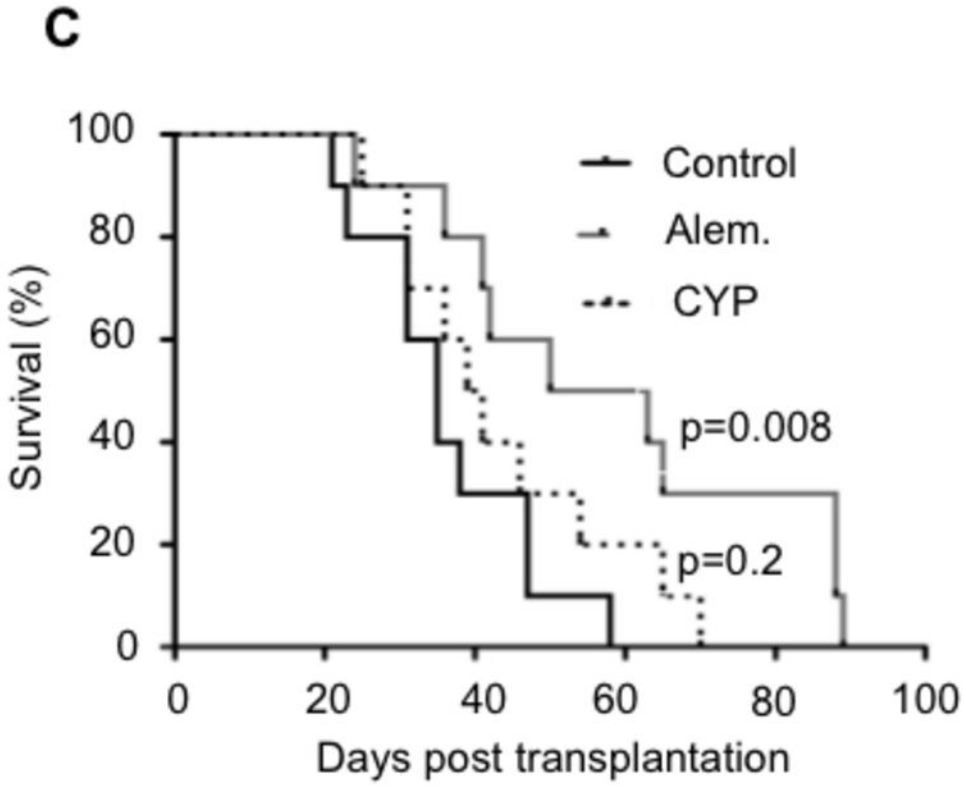
C
Survival (%)
100
80
60
40
20
0
Control
Alem.
CYP
p=0.008
p=0.2
0
20
40
60
80
100
Days post transplantation

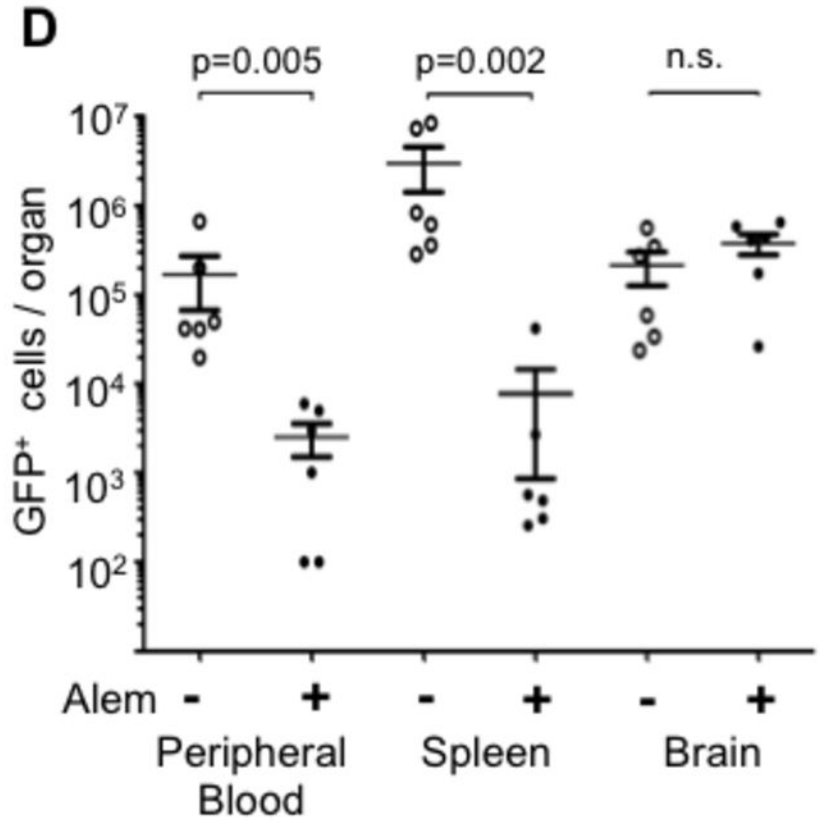
D
p=0.005
p=0.002
n.s.
GFP+ cells / organ
10^7
10^6
10^5
10^4
10^3
10^2
Alem - + - + - +
Peripheral Blood
Spleen
Brain

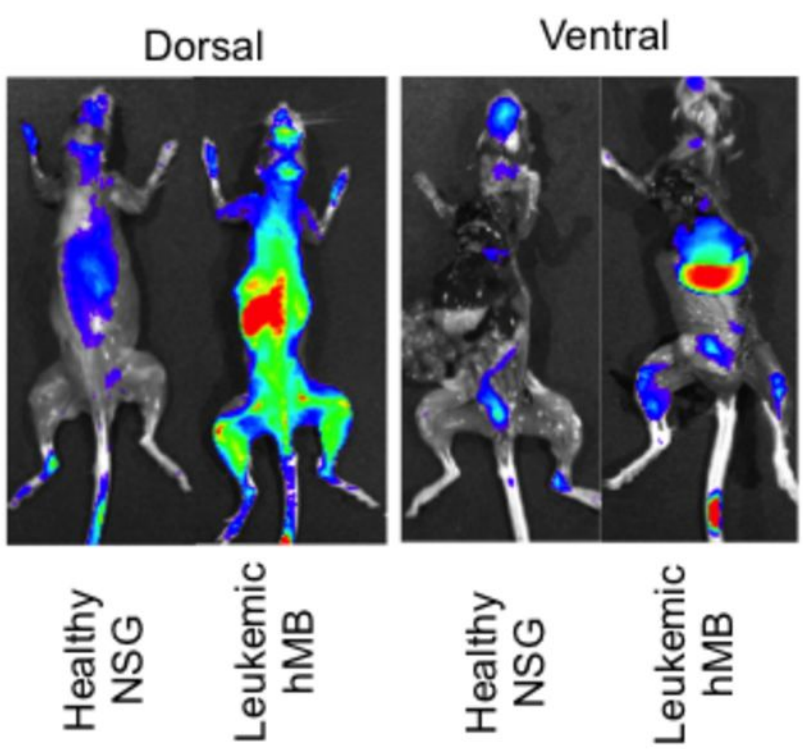
E
Dorsal
Ventral
Healthy NSG
Leukemic hMB
Healthy NSG
Leukemic hMB

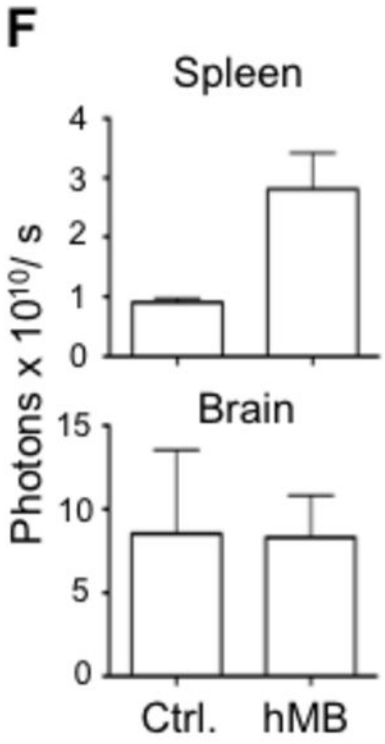
F
Spleen
Photons x 10^10/ s
4
3
2
1
0
Brain
15
10
5
0
Ctrl.
hMB

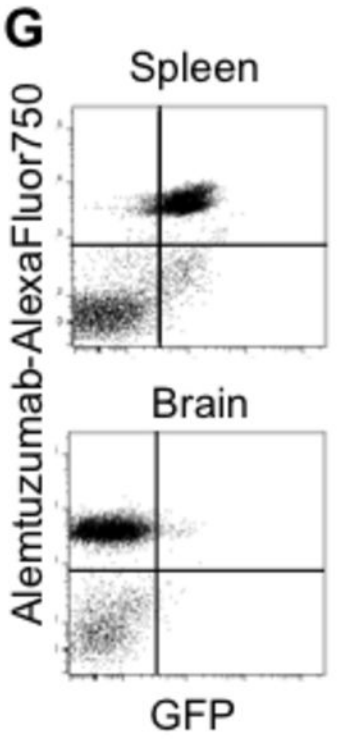
G
Spleen
Alemtuzumab-AlexaFluor750
Brain
GFP